CHINESE JOURNAL OF PHYSICS VOL. 52, NO. 1-II February 2014

Review

Nonperturbative Atomic Dynamics: Population Trapping and Polarization Response in Strong Laser Fields

V. Yu. Kharin,[1,2] A. M. Popov,[1,2,*] O. V. Tikhonova,[1,2] and E. A. Volkova[1]

[1] *Institute of Nuclear Physics, Moscow State University, 119991, Moscow, Russia*
[2] *Physics Department, Moscow State University, 119991, Moscow, Russia*

(Received September 1, 2013)

The population trapping in highly-excited atomic/molecular states under intense femtosecond laser pulse action is studied. Two different mechanisms, namely interference stabilization and Kramers-Henneberger stabilization, are responsible for such a trapping. The implication of the atomic dynamics driven by laser field in the nonperturbative limit of ionization to the determination of the strong-field polarization response is discussed.

DOI: 10.6122/CJP.52.340 PACS numbers: 32.80.Rm, 32.80.Fb, 42.50.Hz

I. INTRODUCTION

Strong-field stabilization (or population trapping) of atoms in high-intensity laser field is the phenomenon that attracts attention of scientists during the last decades. The phenomenon was discovered, first theoretically [1, 2] and only later several attempts were made to observe it in experiments [3–7].

Two main types of atomic stabilization can be distinguished: the interference stabilization (IS) of Rydberg atoms [1, 8, 9] and the Kramers-Henneberger (or adiabatic) one [2, 10]. The physical reason of both types of the stabilization is the formation of so-called "dressed states" that characterize an atom in the presence of a strong field. They appear to differ dramatically from the field-free atomic eigenstates. In the case of interference stabilization the observed ionization suppression can be interpreted as a result of the coherent repopulation of neighboring Rydberg states by Raman transitions and further destructive interference of the transition amplitudes from the repopulated states to the continuum. If the repopulation occurs mostly by Raman Λ-type transitions via continuum, one deals with Λ-type stabilization [1, 8], while the resonant involving of the low-lying bound states corresponds to so-called V-type transitions and V-type stabilization [9]. The threshold of the interference Λ-type stabilization phenomenon can be estimated as

$$\varepsilon_0 \Big/ \omega^{5/3} > 1, \tag{1}$$

where ω is the laser frequency and ε_0 is the amplitude of the laser's electric field strength [1]. For the Ti:Sapphire laser ($\hbar\omega = 1.55$ eV) condition (1) is fulfilled for laser intensities

*Electronic address: alexander.m.popov@gmail.com

$I > I^* \approx 10^{13}$ W/cm^2.

Another mechanism of ionization suppression widely discussed is the Kramers-Henneberger (KH) stabilization [2, 10]. This model of stabilization is usually related to ionization dynamics of non-excited atoms or negative ions. Such a stabilization regime is found to arise due to a significant reconstruction of the energy structure and eigenstates of the system in the presence of the electromagnetic laser field that seems to be rather different in comparison to the repopulation of Rydberg levels caused by Λ- or V-type transitions. In the case of KH stabilization a new "dressed" potential completely different from the field-free atomic one appears in the strong field region, and a system in a laser field reveals essentially new features originating from the formed "dressed atom" – namely, the Kramers-Henneberger atom. Typically the KH stabilization appears to exist in the high-frequency limit $\omega > I_i$ (I_i is the ionization potential) [2, 10]. In [11] it was predicted that in multiphoton regime of ionization the formation of the KH atom will take place only if the laser intensity will exceed the barrier suppression value $I > I_{BSI}$. For most atoms the barrier suppression intensity I_{BSI} is about 10^{14} W/cm^2 or little bit more.

The possibility of IS for the atom in the ground atomic state which is coupled with the continuum by the multiphoton transition was proposed in [12] and studied theoretically in detail in [13]. The key element of such interpretation is the multiphoton resonance of the ground state and a set of high-lying Rydberg states AC Stark shift taking into account, and then the IS of population trapped in excited Rydberg states.

Independently, the same idea of population trapping in Rydberg states was suggested in [14–16] for interpretation of experimental results on the strong – field ionization yields in atoms of noble gases and molecules, respectively. It was found that in a certain intensity range below the saturation intensity, the ion yield would decrease subtly before increasing again. This was explained by the dynamic resonance of the ponderomotively shifted Rydberg states resulting in population trapping. Numerical analysis of the population trapping of Xe atoms was found in qualitative agreement with experimental data obtained by S. L. Chin group [17].

The trapping of population in highly excited Rydberg states was also observed in recent experiments with He atoms irradiated by Ti-Sa femtosecond laser pulse [18]. The authors of this paper proposed the model of the frustrated tunnel ionization. In accordance with this theoretical model the capture to highly excited states take place as a result of the recombination process on parent ion during the turn-off time of the laser pulse caused by the Coulomb interaction with the atomic core. Such a temporal dynamics is in contradiction with the model based on IS phenomenon where the population of excited Rydberg states is found to be pronounced already at the first ramp of the laser pulse as soon as the field amplitude becomes close to its peak value [19].

Recently in was pointed out that population trapping in high-lying Rydberg states can contribute significantly to the polarization response at the fundamental frequency during the self-focusing and filamentation of strong laser pulses [20, 21] and for generation of THz radiation in filaments [22].

The aim of this paper is to present the overview of recent data on the stabilization and population trapping phenomena for different quantum systems in a wide range of laser pulse

parameters and to analyze the contribution of the trapping to the polarization response in the different regimes of ionization.

II. THE MODEL

We performed numerical simulations for a quantum system in single-particle approximation. In the nonrelativistic case, the dynamics of the quantum system in the presence of the electromagnetic wave field is given by the equation

$$i\frac{\partial\psi(\vec{r},t)}{\partial t} = -\frac{1}{2}\nabla^2\psi(\vec{r},t) + V(r)\psi(\vec{r},t) + W(\vec{r},t)\psi(\vec{r},t) \tag{2}$$

where $V(r)$ is the central single-particle potential and $W(\vec{r},t)$ is the operator of the interaction of atomic system with external electromagnetic field. In the dipole approximation, the operator can be represented as

$$W(\vec{r},t) = -\vec{d}\cdot\vec{\varepsilon}(t) \tag{3}$$

where $\vec{\varepsilon}(t)$ is the electric field strength of electromagnetic wave and $\vec{d}$ is the operator of dipole moment. We assume that the electromagnetic wave is linearly polarized and vector ε is directed along the z axis. We also assume that the laser pulse has a smoothed trapezoidal shape with duration of edges t_f and duration of plateau t_p. In the calculations, the durations of edges are several periods of the wave electric field $T = 2\pi/\omega$. Different frequencies of laser radiation from mid IR to UV band corresponding to various regimes of photoionization were under the study. The technique of numerical integration of the time-dependent Schrödinger equation (TDSE) was discussed in detail in [23].

III. DISCUSSION

III-1. Stabilization of atoms in Ti-Sa laser field

Let us discuss first our recent investigations of the dynamics of a Hydrogen atom in low-frequency *Ti-Sa* laser pulses performed by direct numerical solution of the TDSE with the atom-field interaction. Initially the atom is supposed to be in its ground state. The main result obtained in these calculations is presented in Fig. 1 and demonstrates the nonmonotonous dependence of the ionization and excitation [38] probabilities of the Hydrogen atom versus laser intensity. Both curves are seen to reveal a lot of maxima and minima changing each other with each ionization minimum being accompanied by maximum of the excitation and enhancement of trapping the population in high-lying Rydberg states. The maxima observed on the excitation curve are seen to be separated by approximately the same value of laser intensity equal to $\Delta I \approx 2.25 \times 10^{13}$ W/cm^2, which exactly corresponds to the condition that the ponderomotive shift of the ionization threshold $U_{pond} = \varepsilon_0^2/4\omega^2$ changes the photon energy $\hbar\omega$, $\Delta U_{pond} = \omega$. A single oscillation of the excitation probability is presented in details in Fig. 2. To understand the physical reason of such behavior observed

for the excitation it is very useful to analyze the energy spectrum of photoelectrons obtained for intensities corresponding to the maximum and minimum on the curve on Fig. 2. The typical photoelectron spectrum demonstrates a lot of ATI peaks separated by $\hbar\omega$. The main change of the spectrum with growing laser intensity consists in a shift of the positions of the ATI peaks to lower energies and the occurrence of the channel closing effect [24]. Fig. 3 demonstrates the dependence of positions of several first ATI peaks on the peak laser intensity. The channel closing is clearly demonstrated and the change of the multiphoton order of the ionization process is seen to take place as soon as the peak laser intensity is increased by 2.25×10^{13} W/cm^2. As can be seen from Fig. 3 the intensity $7.5 \cdot 10^{13}$ W/cm^2 providing almost the maximum of excitation probability corresponds to the case just after closing of the 12-th channel when 13 photons are needed to be absorbed to go to the continuum. In this situation the energy of the first ATI peak is little smaller 1.5 eV and absorption of 12 photons leads to the transition to closely-situated high-lying Rydberg states that can be efficiently populated. In contrast, for laser intensity $9 \cdot 10^{13}$ W/cm^2 the 13 photon transition to the continuum provides the first ATI peak at the energy ≈ 0.5 eV and the absorption of 12 photons or less gives the possibility to populate only low-lying states with binding energy around 1 eV and rather low principal quantum numbers.

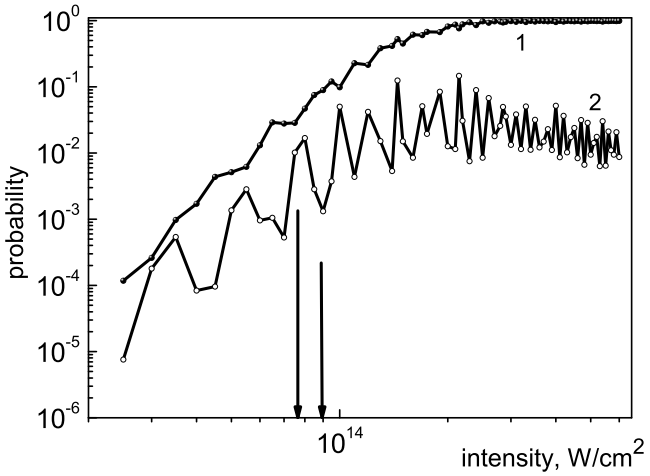

FIG. 1: Probabilities of ionization (1) and excitation (2) of a Hydrogen atom in dependence on the laser intensity for the Ti-Sa laser for the smoothed trapezoidal pulse with ramps and plateau durations of two and ten optical cycles, correspondently. The arrows label the intensity values of 7.5×10^{13} W/cm^2 and 9×10^{13} W/cm^2, corresponding to the maximum and minimum values of excitation probability.

The scheme of the multiphoton transitions into the continuum and possible excitation channels is presented in Fig. 4. Since for intensity $9 \cdot 10^{13}$ W/cm^2 there are only several bound state resonantly coupled with the ground one, the excitation probability is expected

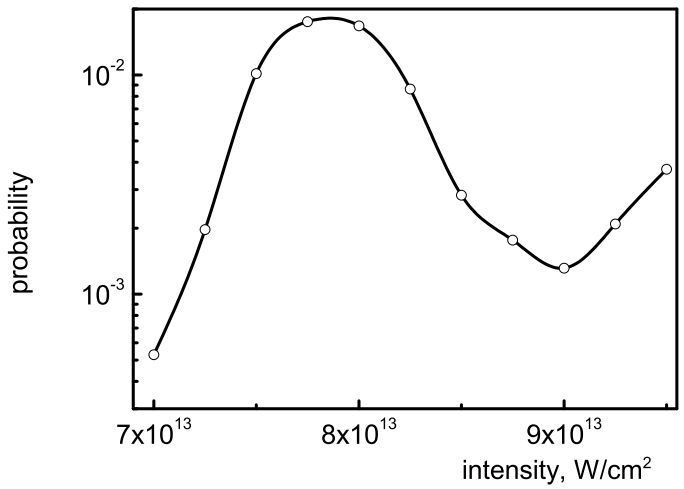

FIG. 2: The detailed structure of one oscillation of the excitation probability versus the laser intensity.

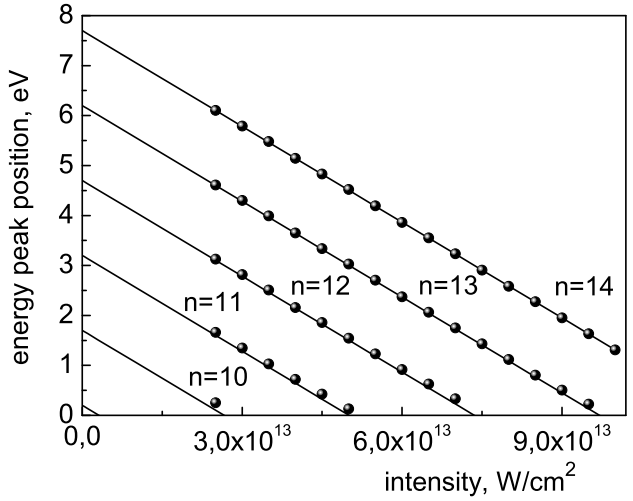

FIG. 3: Energies of several first ATI peaks of the photoelectron spectra in Hydrogen in dependence on the laser intensity. Solid curves correspond to the theoretical calculations taking into account the Stark shift of the continuum boundary.

to be suppressed in this case. Indeed, Fig. 5 demonstrates the dramatic difference of the population of excited states for the two considered laser intensities. For intensity $7.5 \cdot 10^{13}$ W/cm^2 the high-lying Rydberg states with $n = 7$–10 are predominantly populated and the

total probability of excitation appears to be much higher than in the case of intensity $9 \cdot 10^{13}$ W/cm^2 when only several bound states with $n = 3$–5 are found to be populated but with relatively small probability. As a result, the multiphoton resonance coupling between the ground state and a band of close neighboring high Rydberg levels is found to be accompanied by dramatic enhancement of excitation and trapping the population in Rydberg states. The reason of the observed population trapping consists in the repopulation of the resonantly coupled Rydberg band by Raman Λ - type transitions via the continuum that are very efficient in a strong field and results in the significant suppression of the ionization process. The evidence of the found Λ - type transitions is clearly demonstrated by Fig. 6, where the distribution of the bound states over angular momentum is presented for two laser intensities corresponding to two local maxima of the excitation probability. For lower of the two intensities the 12-photon absorption and further Λ - type transitions result in the predominant population of states with only even orbital numbers while for intensity 10^{14} W/cm^2 13 photon are needed to excite the high-lying Rydberg states and a set of odd orbital states are found to be mainly populated due to Λ - type transitions.

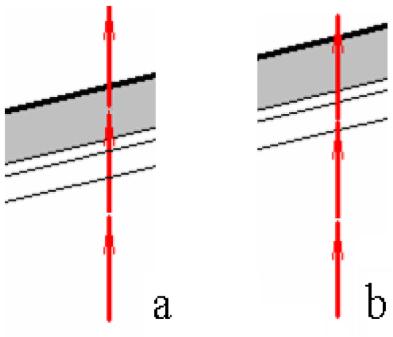

FIG. 4: The scheme of multiphoton transitions into the continuum for intensities 7.5×10^{13} W/cm^2 and 9×10^{13} W/cm^2 corresponding to high (a) and low (b) level of excitation probabilities.

It should be emphasized that the observed enhancement of the excitation means the suppression of ionization and is seen as non-monotonous character and a number of local minima on the dependence of the ionization probability on the laser intensity. Moreover, in a strong field limit the residual bound probability appears to remain at several percents providing the asymptotic value of the ionization probability less than unity. It is also important that the population of excited Rydberg states is found to be pronounced already at the first ramp of the laser pulse as soon as the field amplitude becomes close to its peak value. This fact is clearly demonstrated by Fig. 7. It is seen that rather small part of the population comes back to the bound states during the turn-off of the pulse.

Similar simulations were performed for a single-electron atom with the ionization potential $I = 7.58$ eV, which corresponds to that of silver atom. The single-electron model of a silver atom was discussed in detail in [11, 23]. The probabilities of ionization and excitation as functions of the Ti:Sa laser intensities below the barrier-suppression ionization threshold ($I < I_{BSI} \sim 10^{14}$ W/cm^2) are presented at Fig. 8. For weak fields, when the Stark

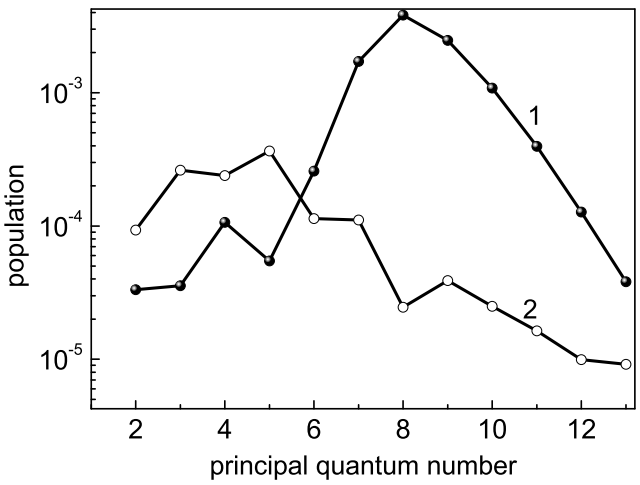

FIG. 5: The population of Rydberg states of the Hydrogen atom with different principal quantum numbers obtained for the laser pulse with ramps and plateau durations of two and ten optical cycles correspondently with peak intensities 7.5×10^{13} W/cm^2 (1) and 9×10^{13} W/cm^2 (2).

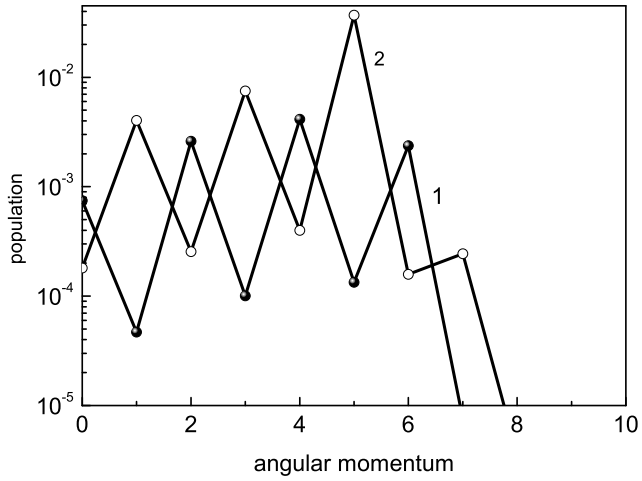

FIG. 6: Distribution of population all bound states in the angular momentum arising after interaction with a laser pulse with ramps and plateau durations of two and ten optical cycles and with peak intensities (1) 7.5×10^{13} W/cm^2 (1) and (2) 9×10^{13} W/cm^2 (2).

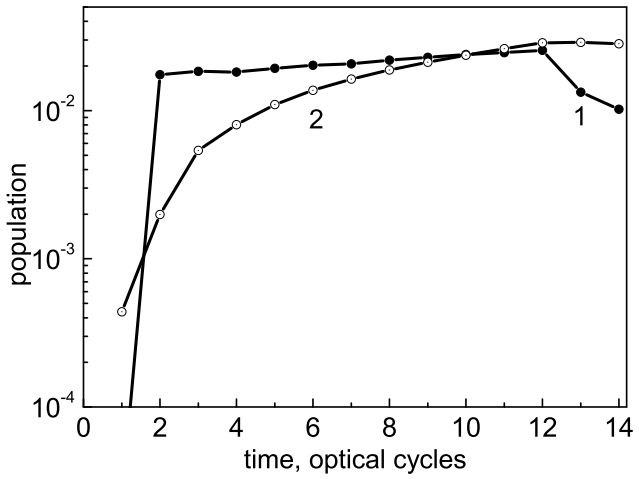

FIG. 7: The temporal population of the excited Rydberg states (1) and continuum (2) for the laser pulse with ramps and plateau durations of two and ten optical cycles correspondently with peak intensity 7.5×10^{13} W/cm^2.

shift of the continuum can be neglected, the ionization is six-photon. In the intensity range below 5×10^{12} W/cm^2, the obtained dependences correspond to the lowest perturbation theory order. For stronger fields ($I \geq 10^{13}$ W/cm^2), the dependences demonstrate the nonmonotonous behavior. The probability of excitation is found to be an oscillating function of the laser intensity with period $\Delta I \approx 2.2 \times 10^{13}$ W/cm^2 that almost coincide with the period found for Hydrogen atom. The value of excitation probability w^* was found to change from 0.02 to 0.3 in the intensity range 10^{13}–10^{14} W/cm^2. For a silver atom in the Ti:Sapphire laser field, the Keldysh parameter is $\gamma = 1$ for a radiation intensity of $\sim 3.5 \times 10^{13}$ W/cm^2. Therefore, even for $\gamma \leq 1$ (tunneling ionization regime), the role of the excited states of the atomic spectrum is important. The distribution of the bound states over angular momentum for different values of laser intensity is similar to that found for Hydrogen atom and clearly proves the existence of Λ - type transitions being responsible for the stabilization.

Thus, the evidence of the interference stabilization in the Ti – Sa laser field was confirmed and the trapping of population in highly-excited Rydberg states due to Λ - type transitions was found. The multiphoton resonance coupling between the ground and a set of high-lying states was demonstrated to result in the suppression rather than the enhancement of ionization as it could be properly expected. Recent experimental data on population trapping in Rydberg states in Helium atoms [25] are found to be in agreement with theory of interference stabilization.

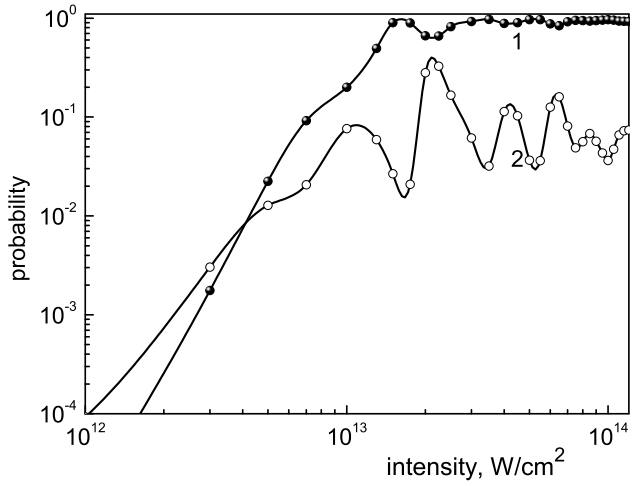

FIG. 8: Ionization (w_i) and excitation (w^*) probabilities for the silver atom as functions of the laser radiation intensity for a Ti-Sa laser pulse with ramps and plateau durations of two and ten optical cycles correspondently.

III-2. Stabilization of atoms in mid IR laser field

The calculations were performed for a Silver atom and for the mid-IR field with the photon energy $\hbar\omega = 0.4$ eV. The laser pulse had a smoothed trapezoidal shape with front and plateau durations $t_f = 2T$ and $t_p = 5T$, respectively. For the defined value of the laser frequency the pulse duration was ≈ 90 fs, that is even more in comparison with the pulse durations of the Ti-Sa laser used in previous sections.

The probabilities of the ionization $w_i(I)$ and excitation $w^*(I)$ of atomic states calculated by the end of the laser action are presented in Fig. 9. First, we would like to note, that in the case under consideration the intensity is below the barrier suppression limit. As the Keldysh parameter $\gamma = \omega\sqrt{2I}/\varepsilon$ is equal to unity for the laser intensity $I \approx 4 \cdot 10^{12}$ W/cm^2, almost all the calculations were performed in the tunnel (but not above barrier) regime of ionization. Nevertheless, the resonances on the dependence $w^*(I)$ are still pronounced. The probability to find the atom in excited states is rather high and reaches the value up to 5 – 6 percents for the intensity range 2 – 3 10^{13} W/cm^2. All this population is trapped in highly excited (Rydberg) states coupled with the continuum by single photon transitions. This effect is similar to that observed experimentally in [16, 18, 25]. The reason of the observed population trapping for mid IR frequency range also consists in multiphoton resonance population of the Rydberg states near the continuum boundary [39] and further repopulation of these states by Raman Λ - type transitions via the continuum that are very efficient in a strong field and result in the significant suppression of the ionization process. The proof of the found Λ - type transitions is clearly demonstrated by Fig. 9 and Fig. 10, where the distributions of the bound states over principal quantum number and angular

momentum are presented for two laser intensities corresponding to two local maxima of the excitation probability. For the intensity of 2×10^{13} W/cm^2 the even-photon absorption and further Λ - type transitions result in the predominant population of bound states with only even orbital quantum numbers while for intensity 2.7×10^{13} W/cm^2 odd - photon are needed to excite the high-lying Rydberg states and a set of odd orbital states are found to be mainly populated due to Λ - type transitions. In the case of the intermediate value of the laser intensity 2.2×10^{13} W/cm^2 the multiphoton resonance between the ground and the group of high-lying Rydberg states is not pronounced that results in the significant decrease of the population of bound states near the continuum boundary. We should also note, that the population is trapped only in the states with binding energy less than $\hbar\omega$.

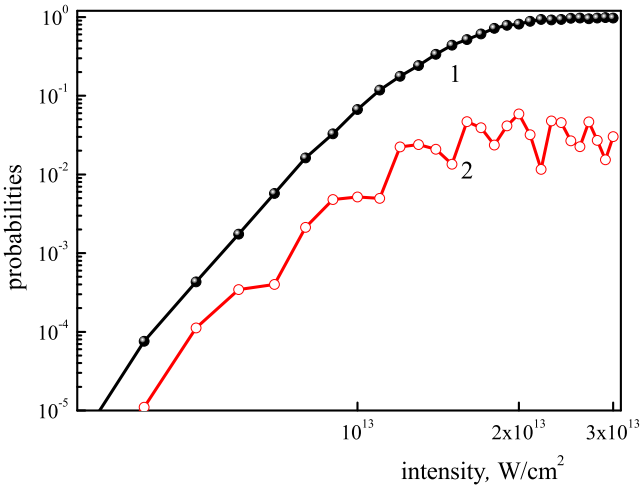

FIG. 9: Probabilities of ionization (1) and excitation (2) of a silver atom in dependence on the laser intensity of mid – IR laser pulse ($\hbar\omega = 0.4$ eV) with ramps and plateau durations of two and five optical cycles.

III-3. Interference stabilization of heteronuclear molecules

An interesting question that hasn't been studied yet in detail and remains still open is whether the interference stabilization against dissociation is possible for molecules and what are the conditions for dissociation suppression to take place. Since the interference stabilization is strongly accompanied by the repopulation of highly excited levels, it is also very important to investigate the dynamics of the bound vibrational wave packet formed in a presence of a strong field.

Due to the laser parameters chosen in our calculations we used the Born-Oppenheimer approximation with only one (ground) molecular potential surface. The time-dependent Schrödinger equation for the nuclear subsystem of the molecule interacting with the laser

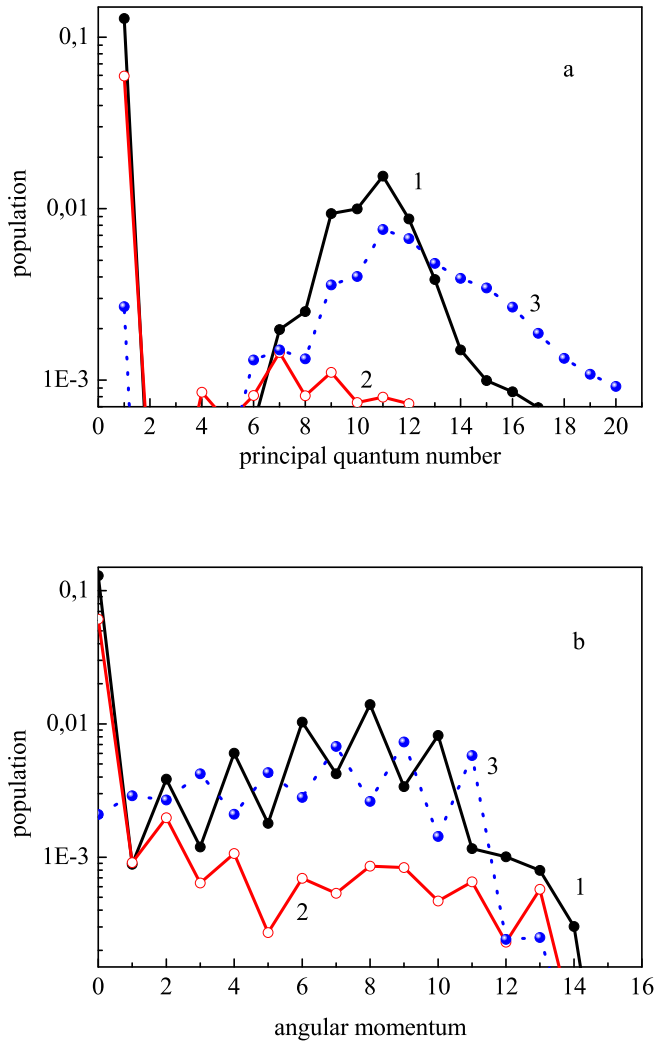

FIG. 10: Distribution of population of all bound states over the principal quantum numbers (a) and the angular momentum (b) arising after interaction with a mid – IR laser pulse ($\hbar\omega = 0.4$ eV) with ramps and plateau durations of two and five optical cycles and with peak intensities (1) 2×10^{13}, (2) 2.2×10^{13}, (3) 2.7×10^{13} W/cm^2.

pulse can be written in the dipole approximation as follows:

$$i\hbar\frac{\partial\psi(\vec{R},t)}{\partial t} = -\frac{\hbar^2}{2\mu}\Delta\psi(\vec{R},t) + \left[V^{(eff)}(R) - q\vec{\varepsilon}(t)\vec{R}\right]\psi(\vec{R},t). \quad (4)$$

Here R is the internuclear distance, μ stands for the reduced mass of the system; $V^{(eff)}(R)$ is the effective potential determining vibrational motion; ε is the linearly polarized laser field,

q is the effective charge of the system which determines the dipole moment of the nuclear subsystem in the own frame of reference of the molecule. In our approach we consider the direct action of the laser field on the nuclear subsystem of the molecule without involving any electron transitions. To describe the potential energy of interaction, the Morse potential curve has been chosen.

$$V^{(eff)}(R) = D\left(\exp\left(-2\alpha\frac{R-R_0}{R_0}\right) - 2\exp\left(-\alpha\frac{R-R_0}{R_0}\right)\right). \tag{5}$$

Here D denotes the dissociation potential; R_0 is the equilibrium internuclear separation, α is the steepness of the potential curve which provides the value of the bottom vibrational quantum $\hbar\Omega \approx 0.1$ eV. In our calculation we took $R_0 = 2.5$ Å, $D = 1.3$ eV, $\alpha = 5$, $\mu = 16$ at. units, $q = 1$.

Following to [26] the equation (4) has been solved numerically with the initial condition corresponding to the superposition of two rather highly-excited vibrational states in the potential (5) and zero initial rotational quantum number:

$$\psi|_{t=0} = \frac{1}{\sqrt{2}}\left(\phi_{v=37}(R) + \phi_{v=39}(R)\right). \tag{6}$$

We assumed the laser pulse envelope had smoothed trapezoidal shape and the energy of laser quantum $\hbar\omega$ equal to 0.1 eV. These parameters correspond to single-photon coupling of each of initially populated states with the vibrational continuum. The laser intensity is chosen not to be very high to provide the validity of the single potential surface approximation.

One of the most interesting results obtained in our calculations consists in the suppression of the dissociation process of the molecule found in a strong field regime. The observed dependence of dissociation probability on the laser intensity is presented on Fig. 11 (solid curve). For high intensities the dissociation probability is found to deviate dramatically and appears to be much lower in comparison to predictions of the generalized perturbation theory (dashed curve). The obtained dissociation probability seems to tend to the saturation at the level less than unity. The physical nature of the found stabilization phenomenon is also supposed to arise from the interference stabilization mechanism. To demonstrate this fact more evidently the dissociation probability of the system is calculated in dependence on time during the laser pulse action for various laser intensities and is presented on Fig. 12. Since two highly excited states are populated initially, in a weak field regime we normally see the linear growth of dissociation probability with time accompanied by some oscillations corresponding to the energy difference between these two states. This result obtained in a weak field case is fully consistent with the perturbation theory. However for intensities above 4×10^{12} W/cm^2 the dynamics of dissociation process changes and is found to be characterized by the bi-exponential decay due to transitions into vibrational continuum (see curves 3, 4). This fact is a clear evidence of the strong reconstruction of the eigenstates of the system in a presence of the strong field and the formation of the "dressed" states. Some of these states appear to be rather resistant to the dissociation process. This picture is very similar to the phenomenon of interference stabilization observed in the case of ionization of Rydberg atoms.

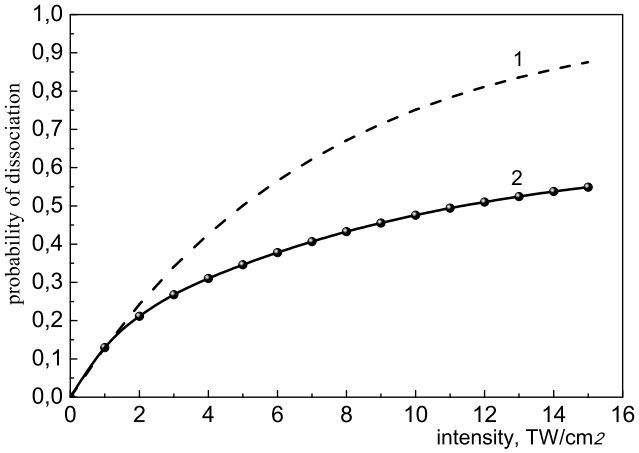

FIG. 11: Probability of dissociation of the molecule as a function of laser intensity. Generalized perturbation theory (1) and numerical TDSE solution (2).

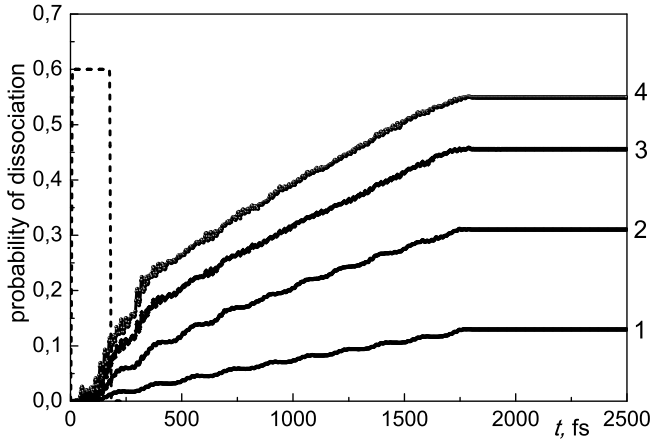

FIG. 12: Probability of dissociation of the molecule as a function of time for different laser intensities: 1 TW/cm^2 (1), 4 TW/cm^2 (2), 9 TW/cm^2 (3), and 15 TW/cm^2 (4). The pulse envelope is presented as dashed curve.

The observed dissociation suppression is found to be accompanied by the trapping of the significant part of population in bound vibrational states. The population of different vibrational states calculated for low and high intensities at the end of the laser pulse is presented on Fig. 13. The peaks located at $v = 37$ and $v = 39$ correspond to initially populated states. As one can see, the field-induced repopulation of various vibrational states is strongly pronounced for high laser intensity. The population of highly-excited (in comparison to initial ones) states results from the Raman Λ-type transitions via the vibrational continuum. The population of lower-lying states is caused by the so-called V-type

transitions and can be characterized by a number of peaks separated by the energy of the laser quantum well seen in the distribution (Fig. 13, circles). Thus, in a strong field regime the suppression of dissociation of a molecule is found to take place due to the interference stabilization mechanism and trapping of population in excited bound vibrational states is observed to result from the Raman Λ- and V-type transitions.

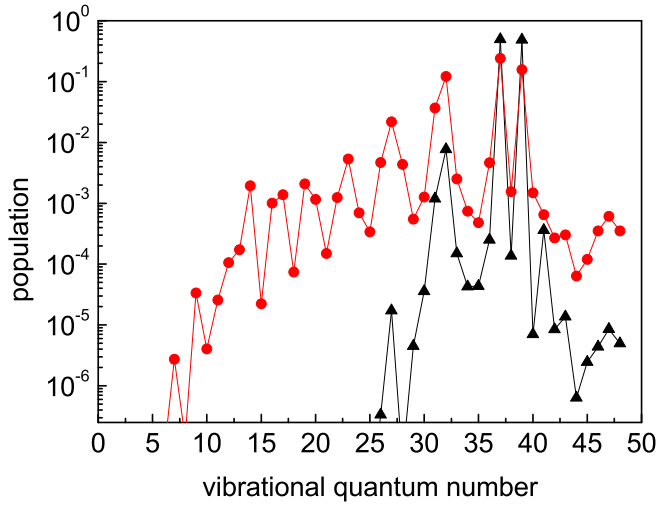

FIG. 13: The population of vibrational bound states calculated at the end of the laser pulse for weak field (laser intensity 0.1 TW/cm^2) – triangles and for strong field (laser intensity 15 TW/cm^2) – circles.

III-4. Kramers-Henneberger regime of stabilization

In this chapter another one type of stabilization of atomic systems in strong laser fields, namely the Kramers – Henneberger (KH), is discussed. This type of stabilization appears to exist for atoms in the ground state in the case of single-photon coupling with the continuum. It should also be noted that, in high-intensity laser fields with a nonperturbative regime of ionization during laser pulse action, one may very tentatively speak of the population of particular atomic states assuming a definite basis set of atomic states of the discrete spectrum and continuum. Use of the basis set of a free atom in this case is, generally speaking, incorrect because a strong radiation field produces a significant modification of atomic states and leads to the formation of a "field-dressed" atom. In the case under consideration these states for a field-dressed atom are represented by those of the Kramers–Henneberger (KH) atom [27, 28]. States of the discrete spectrum in the KH potential may correspond to states of the continuum in the basis set of a free atom and vice versa, states in the continuum of the KH potential may correspond to states of the discrete spectrum of a free atom.

To demonstrate the KH regime of stabilization we analyze the interaction of a silver

atom with UV radiation ($\hbar\omega = 9.0$ eV, $\tau_f = 5T$, and $\tau_p = 10T$), where the ground state and all excited states are coupled to the continuum by single-photon transitions. For this case, the probability of ionization $w_i(I)$ as a function of the radiation intensity is presented in Fig. 14, while the excitation of states in the discrete spectrum can be ignored. An important feature of the $w_i(I)$ curve is the presence of an interval of intensities ($I > I^* \approx 4 \times 10^{15}$ W/cm^2) corresponding to stabilization of the quantum system with respect to the ionization process. In this case, stabilization can be treated in terms of the KH formalism [28] and the threshold of this regime can be determined from the condition $\varepsilon/\omega^2 > a$, where $a = 3$–4 is the characteristic size of a silver atom. In this regime, up to 20% of the population still trapped in the bound ground state.

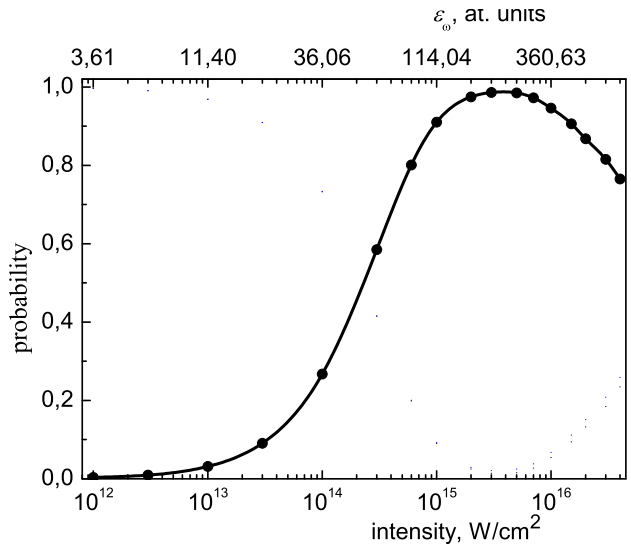

FIG. 14: Plot of the probability of ionization w_i for a model silver atom in the field of UV radiation with photon energy $\hbar\omega = 9.0$ eV and with ramps and plateau durations of five and ten optical cycles.

We should mention also that the KH type of stabilization is also can be observed in the multiphoton limit of ionization in the fields above the barrier-suppression threshold. Such situation was studied in detail in [19]. It seems that in the case of barrier-suppression ionization, the electrons will rapidly (for times on the order of half the optical cycle) transfer to the continuum state, and the residual nonionization (excitation) probability in barrier-suppression fields should be vanishingly small. However, the residual probability to find the atom in the bound (Rydberg) state is still $\sim$ 4–8% in superatomic atomic fields. In this case, unlike intensity range $I < I_{BSI}$ where the strongly nonmonotonic dependence $w^*(I)$ was observed, caused by the closing of ionization channels and the resonance population of a group of Rydberg states stable with respect to ionization, the dependence of the population trapped in Rydberg states $w^*(I)$ on the laser intensity in barrier-suppression fields behaves differently (see Fig. 15). In this intensity range, the dependence is smooth and resonances

are absent. The analysis of photoelectron energy spectrum [11, 19] demonstrates the absence of the channel closing effect and the coincidence of the peaks position with that following from the assumption that the "dressed" atom exists in a form of KH atom.

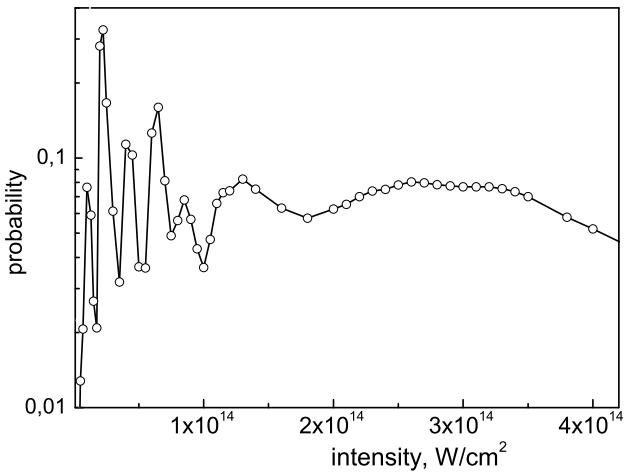

FIG. 15: Dependence of the excitation probability of a model silver atom on the Ti-Sa laser intensity in fields lower and higher than the barrier-suppression threshold I_{BSI} with ramps and plateau durations of two and ten optical cycles correspondently.

Thus, in barrier-suppression fields ($I > I_{BSI}$) the system is stabilized: a considerable part of the electron density forms a Rydberg wavepacket stable with respect to ionization. However, the stabilization mechanism of an atom in barrier-suppression fields differs from the interference mechanism. It is known that the spectrum of atomic states in a superatomic-intensity electromagnetic field considerably changes and a dressed atom is produced in the form of a KH atom [28]. In the case of the silver atom, as mentioned above, superatomic intensities are achieved above $I_{BSI} \approx 10^{14}$ W/cm^2.

III-5. Polarization response of a quantum system in a nonperturbative limit of interaction with a laser field

The creation of laser sources more than fifty years ago made it possible to reach the intensities $10^{10} \div 10^{12}$ W/cm^2 in the optical frequency band and to observe a lot of nonlinear effects. To understand the physics of these effects it is necessary to determine the polarization response of the medium to an external high-intensity electromagnetic field. For example, to describe the phenomenon of the self-focusing of electromagnetic radiation the value of the response at the frequency of the acting field should be calculated. The generation of harmonics of the incident radiation is determined by the response at the harmonics of the fundamental frequency. It is important to note that for the above mentioned intensity range the electric field in an electromagnetic wave is two or three orders

of magnitude smaller than the atomic field value. Therefore, to perform the analysis of the atomic response to the external action, it is possible to use the quantum mechanical perturbation theory and the expansion of the response in powers of the field. For example, to describe correctly the self-focusing effect of the radiation, it is necessary to take into account the nonlinear susceptibilities of all odd-orders (except the first one) of the fundamental frequency. If the perturbation theory is valid the main contribution to the nonlinear response gives the cubic susceptibility of the medium. Nonlinear susceptibilities of the fifth and higher odd orders give additional (small) contribution to the nonlinear response at the frequency of the acting field.

Thus, using the proposed approach, the atomic response at the field frequency can be expressed as a series:

$$d_\omega = \chi(\omega, \varepsilon_\omega)\varepsilon_\omega = \chi^{(1)}(\omega)\varepsilon_\omega + \chi^{(3)}(\omega)\varepsilon_\omega^3 + \ldots, \tag{7}$$

where $\chi^{(1)}(\omega)$ is the linear and $\chi^{(3)}(\omega)$ is the cubic nonlinear susceptibility component, respectively, at the radiation field frequency. Similarly, for analysis of the third-harmonic generation (at the triple frequency), we have

$$d_{3\omega} = \chi(3\omega, \varepsilon_\omega)\varepsilon_\omega = \chi^{(3)}(3\omega)\varepsilon_\omega^3 + \chi^{(5)}(3\omega)\varepsilon_\omega^5 + \ldots \tag{8}$$

where $\chi^{(3)}(3\omega)$ and $\chi^{(5)}(3\omega)$ are the cubic and fifth-order nonlinear susceptibilities, respectively, at the third harmonic frequency. All above mentioned susceptibilities can be calculated in the frames of quantum-mechanical perturbation theory.

The appearance of high-power (terawatt) pulsed lasers capable of generating radiation with electric field strength comparable to (or even greater than) the intra-atomic values and a pulse duration of several tens of femtoseconds makes it of special importance to investigate nonlinear processes in this new range of laser radiation parameters. However, under these conditions, quantum-mechanical perturbation theory is no longer applicable to the description of atomic dynamics in the field of laser radiation and, hence, expansion in powers of the field intensity cannot be used for calculating atomic susceptibilities. Therefore, the determination of atomic response in such a nonperturbative limit is one of the most important problems of modern nonlinear optics and atomic physics.

On the other hand, within a pulse several tens of femtoseconds long, particles in a gaseous medium experience no mutual collisions. This implies that the polarization response of the medium may be calculated by studying the dynamics of a single atom or molecule in the field of a high-intensity ultrashort laser pulse. At present, this problem can be numerically solved from first principles, by the direct integration of a nonstationary Schroedinger equation that describes the dynamics of an atom (molecule) of a gas phase in the electromagnetic wave field [29]. This approach was recently developed in a number of papers [20, 21, 31–33].

The polarization response of an atomic system can be calculated from the wave function of the system $\psi(\vec{r}, t)$ obtained as a result of solution of TDSE:

$$\langle d_z(t) \rangle = -\int r\cos(\theta)\,|\psi(\vec{r}, t)|^2 d^3r, \tag{9}$$

where θ is the angle between the electric field vector $\vec{\varepsilon}(t)$ (oriented along axis OZ) and the electron radius-vector $\vec{r}$. Note that the dipole moment arising in the case under consideration is directed along the radiation polarization vector.

Then, using expansions of $\varepsilon(t)$ and $\langle d_z(t)\rangle$ into Fourier integrals

$$\varepsilon_\Omega = \frac{1}{\sqrt{2\pi}} \int \varepsilon(t) \exp(-i\Omega t) dt, \tag{10}$$

$$d_\Omega = \frac{1}{\sqrt{2\pi}} \int \langle d_z(t)\rangle \exp(-i\Omega t) dt \tag{11}$$

it is possible to determine the spectral expansion $d_\Omega(\varepsilon_\Omega)$ of the polarized response, calculate from first principles the susceptibility at various frequencies, determine the domains of applicability of the method of response expansion in powers of the field, and analyze contributions to the response from various atomic states in the discrete spectrum and continuum for the strong field limit, where the expansion in powers of the field is definitely incorrect.

It is more convenient to perform the calculations of the atomic response to apply the Ehrenfest theorem and to calculate first the acceleration

$$\langle a_z(t)\rangle = -\varepsilon(t) - \left\langle \frac{\partial V}{\partial z} \right\rangle, \tag{12}$$

and then using the expression $d_\Omega = a_\Omega/\Omega^2$ to obtain the spectral component of the polarization response d_Ω.

Let us first consider the results of calculations of the nonlinear susceptibility of silver atoms in IR field with a photon energy of $\hbar\omega = 1.5$ eV, which approximately corresponds to the radiation of a Ti:Sapphire laser. For this analysis, the wavefunction $\psi(\mathbf{r}, t)$ determined by direct numerical integration of the nonstationary Schroedinger equation (1) has been used to calculate the acceleration via Eqs. (12) for various laser intensity values.

Figure 16 demonstrates the typical results of these calculations for two radiation intensity values. Note that the case of a lower intensity (3×10^{12} W/cm^2) corresponds to a regime of perturbation theory where the ionization and excitation probabilities are much less unity. The opposite situation takes place for a greater intensity (1.5×10^{13} W/cm^2), where the ionization probability increases up to 0.90. As a result, the acceleration amplitude increases with time and application of the perturbation theory for calculations of the polarization response becomes impossible.

The functions were decomposed into Fourier integrals. Figure 17 shows these spectral expansions for two values of laser intensity. The curves reveal clearly pronounced maxima at Ω values corresponding to odd harmonics of the laser radiation frequencies, $\Omega_{2n+1} = (2n + 1)\omega$, $(n = 0, 1, 2, \ldots)$. Then, it is possible to calculate nonperturbatively the polarization response at $\Omega_{2n+}1$, and to determine the limit of the validity of the perturbation theory.

Figure 18 shows a plot of the polarization response d_ω at the fundamental frequency versus spectral value of the electric field ε_ω (or radiation intensity I). In relatively weak fields, when the atom under laser action remains predominantly in the ground state, the

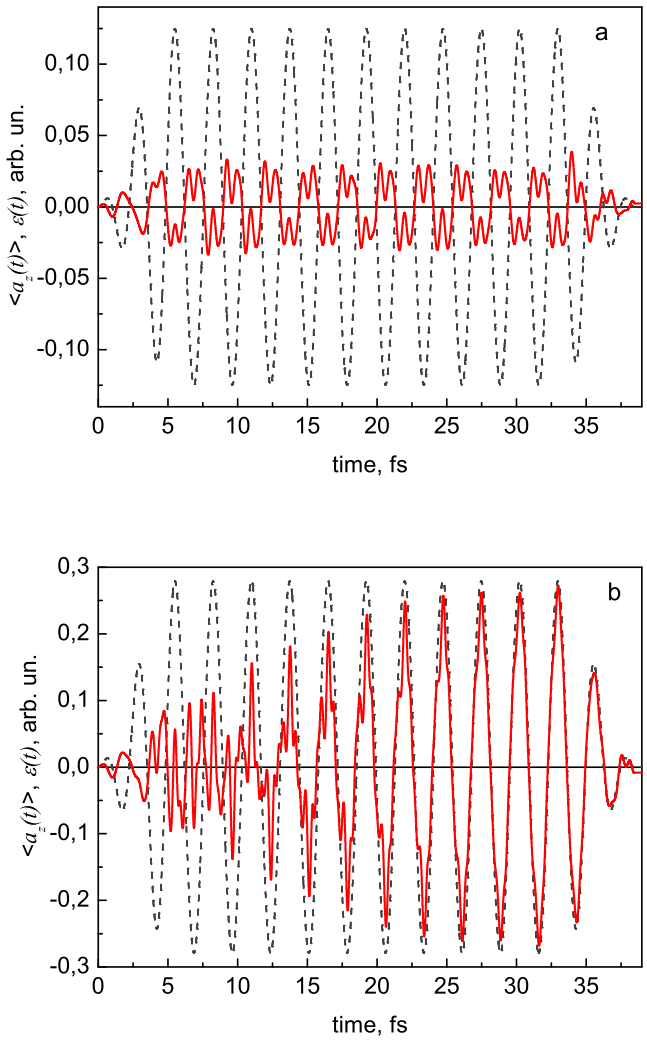

FIG. 16: Temporal variation of the (solid curves) quantum-state average acceleration of a model silver atom and (dashed curves) electric field strength ε (b) for radiation with photon energy $\hbar\omega = 1.5$ eV and intensity (a) 3×10^{12} and (b) 1.5×10^{13} W/cm^2.

obtained dependences are adequately described by expression (7), which take into account the linear and cubic terms in powers of the field strength. However, as the field intensity increases above 5×10^{12} W/cm^2, the polarization response saturates, then decreases, and eventually changes sign to become negative. This behavior implies that, as the radiation intensity increases, the properties of the medium change from focusing to defocusing, which leads in practice to filamentation of the radiation.

The detailed analysis of the contribution of different atomic states to the nonlinear

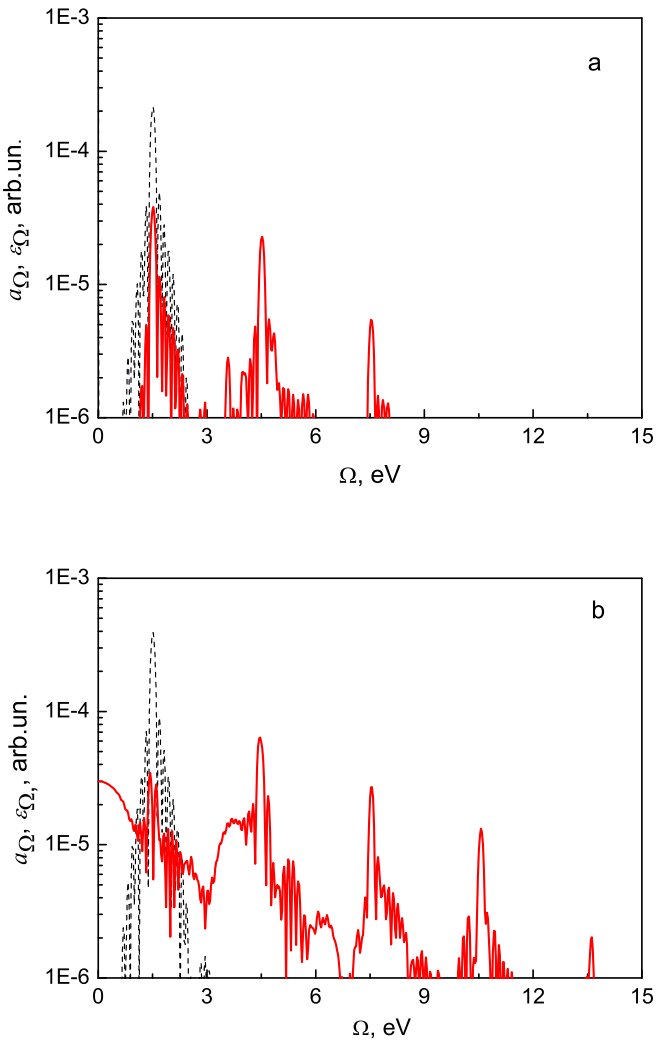

FIG. 17: Spectral expansions of electron acceleration (solid curves) during laser pulses with photon energy $\hbar\omega = 1.5$ eV and intensity (a) 3×10^{12} and (b) 1.5×10^{13} W/cm^2. Dashed curves correspond to the spectral expansion of a laser pulse.

atomic susceptibility $\chi(\omega, \varepsilon_\omega)$ plotted in Fig. 19 (curve 1) was performed in [31, 32]. It was found that, under the studied conditions, the contribution from low-lying excited atomic states to the total atomic susceptibility is negligibly small and the $\chi(\omega, \varepsilon_\omega)$ is determined mainly by free electron plasma component and population trapped in high-level Rydberg states. Hence, saturation of the response and the change in its sign is undoubtedly related to the photoionization and stabilization of highly excited atomic states. Which particular mechanism of trapping atoms in the highly excited states (interference stabilization or

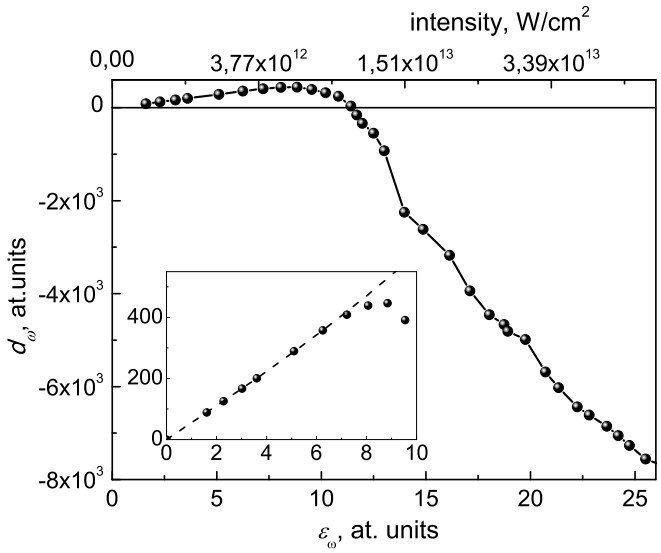

FIG. 18: Plot of the polarization response d_ω of a model silver atom at the fundamental frequency ω vs spectral value of the electric field ε_ω (or radiation intensity I). The inset shows the region of small fields on a greater scale, which can be used to determine the limits of applicability of the expansion of polarization in powers of the field strength. Dashed line corresponds to Eq. (7) that takes into account the linear and cubic terms of expansion.

KH atom formation) is not important due the fact that Rydberg atoms contribute to the response like the continuum states.

As the susceptibility of free electron and high-lying Rydberg states is $\chi_e(\omega) = -1/\omega^2$ [34] and increases dramatically in low-frequency domain the role of the effects of the ionization and population trapping is expected to grow up significantly in mid-IR frequency band and dominate in comparison with the contribution of Kerr effect even for significantly low value of ionization probability. The calculated dependence of the susceptibility at the fundamental mid IR frequency $\chi(\omega, \varepsilon_\omega) = d_\omega(\varepsilon_\omega)/\varepsilon_\omega$ is shown in figure 20. In relatively weak laser fields up to 5×10^{12} W/cm^2, when the atom remains dominantly in the ground state, the value of susceptibility is approximately constant and corresponds to the static value for the silver atom. However, for higher intensities one first observes the decrease of the polarization response, after which it changes sign and becomes negative for intensities larger than 8×10^{12} W/cm^2. The change of the response sign can be caused by the population of high-lying Rydberg and continuum states only. Indeed, the susceptibility of a free electron gas (collisionless plasma) per one electron, is determined by the expression $\chi_e(\omega) = -1/\omega^2$. This value for a photon of mid-IR laser radiation with $\hbar\omega = 0.4$ eV is more than two orders of magnitude larger than the linear atomic susceptibility $\chi^{(1)}(\omega)$ of a silver atom. Therefore, even at a degree of gas ionization of about 1 %, the contribution of free electrons in the continuum to the polarizability of the medium is expected to be dominant. That is the situation observed in our calculations: the ionization probability per

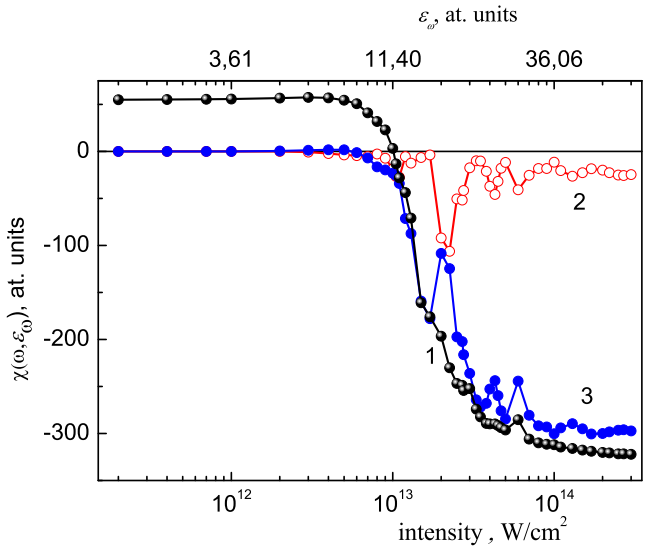

FIG. 19: Plots of the (1) total susceptibility $\chi(\omega, \varepsilon_\omega) = d_\omega(\varepsilon_\omega)/\varepsilon_\omega$ of a model silver atom at the radiation field frequency, (2) contribution due to Rydberg atoms, and (3) contribution due to electrons in the continuum and low-lying excited atomic states vs. spectral value of the electric field ε_ω (or radiation intensity I).

pulse for silver atoms at the intensity of 8×10^{12} W/cm^2, when the response changes the sign, is about ~ 0.01.

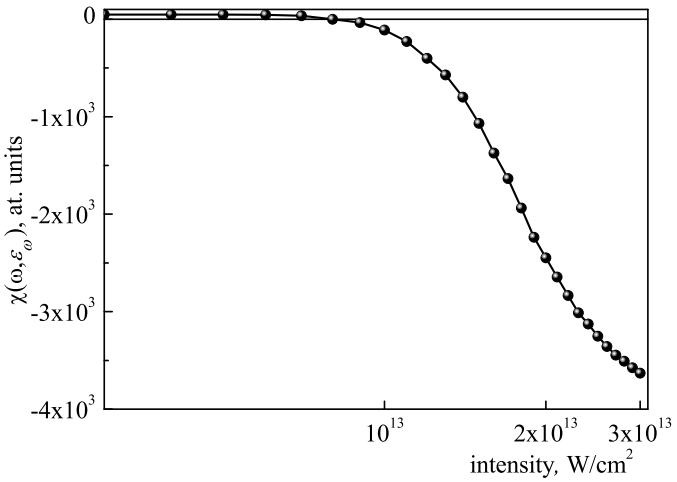

FIG. 20: The dependences of the susceptibility of model silver atoms $\chi(\omega) = d_\omega(\varepsilon_\omega)/\varepsilon_\omega$ at the fundamental frequency for the mid IR laser radiation.

Another situation appears to exist for high-frequency (UV) radiation, when the ground state coupled to the continuum by single-photon transitions. Figure 21 shows the results of calculating the total susceptibility $\chi(\omega, \varepsilon_\omega)$ and the contributions from neutral atoms and electrons in the continuum for the case under consideration. Important feature of the obtained dependence is that the atomic susceptibility is negative even in weak fields and its absolute value is even greater than that of free electrons. Indeed, for single-photon transitions between the ground state and continuum, the linear atomic susceptibility $\chi_g^{(1)}(\omega)$ is given by

$$\chi_g^{(1)}(\omega) \approx \int |d_{Eg}|^2 \cdot \frac{2(E - E_g)}{(E - E_g)^2 - \omega^2} dE, \tag{13}$$

where $E_g < 0$ is the atomic ground-state energy and E is the electron energy in the continuum. As can be seen from (13), a narrow energy interval near $E = E^* = \omega - |E_g|$ dominantly contribute to the integral. Since the square modulus of a matrix element of the dipole operator $|d_{Eg}|^2$ for a Coulomb spectrum is a monotonically decreasing function of the energy, the integral in Eq. (13) is negative and, hence, $\chi_g^{(1)}(\omega) < 0$. A detailed analysis of susceptibility (13) for a hydrogen-like system was carried out in [35]. In particular, for the initial s state of the atom expression (13) can be expanded in the high-frequency limit ($\omega \gg |E_g|$) as

$$\chi_g^{(1)} = -\frac{1}{\omega^2} - \frac{4}{3n^3\omega^4} + \ldots, \tag{14}$$

where n is the principal quantum number of the initial state. In this expansion, the first term describes the susceptibility of the free electron and the second term is an additive, which is also negative and rapidly decreases in absolute value with increasing of laser frequency and principal quantum number of the initial state.

In view of the above considerations, the ionization process and the appearance of free electrons must lead to a growth in susceptibility with increasing intensity in agreement with our calculations (see Fig. 21). In the region of stabilization ($I > I^* \approx 4 \times 10^{15}$ W/cm^2), where the probability of ionization decreases with increasing radiation intensity, the susceptibility keeps growing so as to approach the value corresponding to the susceptibility of free electrons. This implies that the susceptibility of neutral atoms at intensities significantly exceeding the stabilization threshold I^* almost coincides with the susceptibility of free electrons. This behavior of the atomic susceptibility can be explained in the frames of the KH formalism. Indeed, in the region of $I > I^*$, the potential of a field-dressed atom (KH atom) acquires an additional dichotomic structure, the size of which is determined by the amplitude of oscillations of free electrons, $a_e = \varepsilon/\omega^2$, in the electromagnetic wave field. The spatial size of this structure increases with intensity, which leads to a decrease in the potential of ionization of the field-dressed atom, which becomes significantly lower than the photon energy. As a result, oscillations of the atomic electron become quasi-free. The results of our previous analysis of the susceptibility of a field-dressed atom [36] also confirmed that the susceptibility of a KH atom is close to that of a free electron. The significant contribution to the atomic response of the bound states of the KH atom was demonstrated also in recent paper [37].

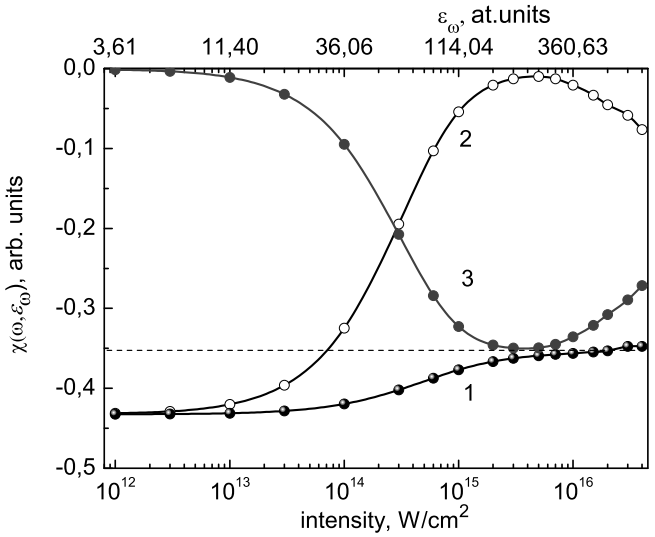

FIG. 21: Plot of the total susceptibility χ_ω at the fundamental frequency (curve 1), contribution due to neutral atoms (curve 2), and contribution due to electrons in the continuum (curve 3) for a model silver atom in the field of UV radiation with photon energy $\hbar\omega = 9.0$ eV (dashed line indicates the level of susceptibility determined by free electrons).

IV. CONCLUSIONS

In conclusion, we have found that population trapping in strong laser field is a sufficiently general phenomenon occurring both in atoms and in molecules. This trapping is the result of ionization (or dissociation) suppression or stabilization phenomenon. Two different types of stabilization were distinguished in our study. One of them, interference stabilization (IS) can be observed either if one prepares in advance atoms or molecules excited to a set of closely located (Rydberg or vibrational) levels in processes of direct multiphoton ionization or dissociation from ground levels. In the last scheme of experiments, under proper conditions, ionization or dissociation can be accompanied by an efficient population of highly excited bound levels, at which the IS effect can occur. Stabilization occurs most efficiently when the multiphoton resonance appears between the ground state of the atom a group of Rydberg states near the continuum boundary. In stronger (barrier-suppression) fields, the atomic spectrum of the system drastically changes, resulting in the disappearance of a nonmonotonic dependence of the ionization probability on the radiation intensity caused by the closing of ionization channels: a dressed atom appears, which is stable with respect to ionization, as follows from the KH formalism.

The nonperturbative strong-field atomic dynamics should be taken into account in determination of the polarization response and atomic susceptibilities. Our numerical calculations of the polarization response clearly demonstrate limitations of the approach based on the quantum-mechanical perturbation theory and on the expansion of this response in

powers of the electric field strength and the introduction of nonlinear susceptibilities of various orders. In the case of IR radiation, the electron dynamics in atoms already at the intensity in excess of 3×10^{12} W/cm^2 has a significantly nonperturbative character and cannot be adequately described by the quantum-mechanical perturbation theory. In particular, in the nonperturbative regime, the most important effects contributing to the polarization response at the fundamental frequency are related to electron transitions from the initial state to the continuum and to the population of high-lying (Rydberg) states. These processes change the sign of the atomic response and are responsible for the filamentation of ultrashort high-intensity laser pulses in various media. Due to the fact that the susceptibilities of Rydberg states of atoms and free electrons are close, it is apparently a very difficult experimental task to reveal contributions related to the ionization and excitation of Rydberg states. In the barrier-suppression regime of ionization, it is convenient to study the problem using a basis set of states of the KH atom. This approach makes it evident the ambiguous character of dividing atomic states into those belonging to states in the continuum and discrete spectrum, since for the dichotomy structure of KH potential, bound states of KH atom seem to be continuum states of field-free atom and vise versa.

Acknowledgments

This work was supported by the Russian Foundation for Basic Research (Grant No. 12-02-00064 and 14-02-31114). Numerical integration of the Schrödinger equation was performed on the SKIF-MGU Chebyshev and Lomonosov supercomputers.

References

[1] M. V. Fedorov and A. M. Movsesian, J. Phys. B: At. Mol. Opt. Phys, **21**, L155 (1988); Sov. Phys. JETP, **68**, 27, (1989).
[2] M. Pont and M. Gavrila, Phys. Rev. Lett., **65**, 2362 (1990).
[3] R. R. Jones, D. W. Schumacher and P. H. Bucksbaum Phys. Rev. A, **47**, R49 (1993).
[4] J. H. Hoogenraad, R. B. Vrijen and L. D. Noordam Phys. Rev. A, **50**, 4133 (1994).
[5] M. P. de Boer, J. H. Hoogenraad et al, Phys. Rev. Lett., **71**, 3263 (1993).
[6] M. P. de Boer *et al.*, Phys. Rev. A, **50**, 4085 (1994).
[7] N. J. von Drutten *et al.*,
[8] M. V. Fedorov, Laser Phys. **3**, 219 (1993).
[9] N. P. Poluektov and M. V. Fedorov, JETP, **90**, 794 (2000).
[10] M. Gavrila, J. Phys. B, 35, 147 (2002).
[11] A. M. Popov, O. V. Tikhonova and E. A. Volkova, J. Phys. B.: At. Mol. Opt. Phys., **32**, 3331 (1999).
[12] Yu. V. Dubrovskii, M. Yu. Ivanov and M. V. Fedorov, Sov. Phys. JETP, **99,** 228 (1991).
[13] A. M. Popov, O. V. Tikhonova and E. A. Volkova, Laser Phys., **10**, 898 (2000); Laser Phys., **20**, 1028 (2010).
[14] A. Talebpour, C. Y. Chien and S. L. Chin, J. Phys. B: At. Mol. Opt. Phys., **29**, 5725 (1996).
[15] A. Talebpour, Y. Liang and S. L. Chin, J. Phys. B: At. Mol. Opt. Phys., **29**, 3435 (1996).

[16] A. Azarm, S. Ramakrishna, A. Talebpour, S. Hosseini, Y. Teranishi, H. L. Xu, Y. Kamali, J. Bernhardt, S. H. Lin, T. Seideman and S. L. Chin, J. Phys. B: At. Mol. Opt. Phys., **43**, 235602 (2010).
[17] A. Azarm, S. M. Sharifi, A. Sridharan, S. Hosseini, Q. Q. Wang, A. M. Popov, O. V. Tikhonova, E. A. Volkova, S. L. Chin, Journal of Physics: Conference Series, **414**, 012015 (2013).
[18] T. Nubbemeyer, K. Gorling, A. Saenz, U. Eichmann and W. Sandner, Phys. Rev. Lett., **101**, 233001 (2008).
[19] E. A. Volkova, A. M. Popov and O. V. Tikhonova, JETP, **113,** 394 (2011).
[20] E. A. Volkova, A. M. Popov, O. V. Tikhonova, Quantum Electronics, **42**, №8, 680 (2012).
[21] E. A. Volkova, A. M. Popov, O. V. Tikhonova, JETP, **116**, 372 (2013).
[22] S. L. Chin, A. Azarm, H. L. Xu, T. J. Wang, M. Sharifi, A. Talebpour, in *Progress in Ultrafast Intense Laser Science,* vol. 8 (PUILS 8), ed Kaoru Yamanouchi, Mauro Nisoli and Wendell T. Hill, III, editors. Springer, Chapter 4, p.79-95 (2012).
[23] A. M. Popov, O. V. Tikhonova and E. A. Volkova, Laser Phys.**, 21,** 1593 (2011).
[24] H. G. Muller, H. B. van Linden Van Den Heuvell, P. Agostini, G. Petite, A. Antonetti, M. Franco, A. Migus, Phys. Rev. Lett., **60**, 565 (1988).
[25] U. Eichmann, A. Saenz, S. Eilzer, T. Nubbemeyer, and W. Sandner, Phys. Rev. Lett., **110**, 203002 (2013).
[26] V. Yu. Kharin, A. M. Popov and O. V. Tikhonova, Laser Phys., **22**, 1693 (2012).
[27] M. V. Fedorov, *Atomic and Free Electrons in a Strong Light Field* (World Scientific, Singapore, 1997).
[28] A. M. Popov, O. V. Tikhonova, and E. A. Volkova, J. Phys. B: At., Mol. Opt. Phys. **36**, R125 (2003).
[29] E. A. Volkova, A. M. Popov, and O. V. Tikhonova, JETP Letters, **94,** 519 (2011).
[30] J. M. Brown, A. Lotti, A. Teleki, and M. Kolesik Phys. Rev. A **84**, 063424 (2011).
[31] P. Béjot, E. Cormier, E. Hertz, B. Lavorel, J. Kasparian, J.-P. Wolf, and O. Faucher Phys. Rev. Lett., **110**, 043902 (2013).
[32] C. Koehler, R. Guichard, E. Lorin, S. Chelkowski, A. D. Bandrauk, L. Berge, and S. Skupin Phys. Rev. A, **87**, 043811 (2013).
[33] A. M. Popov, O. V. Tikhonova and E. A. Volkova, Laser Phys. Lett., **10**, 085303 (2013).
[34] N.B. Delone and V.P. Krainov, *Multiphoton processes in atoms* (Berlin: Springer-Verlag) section 2.4 (1993)
[35] A. A. Krylovetsky, N. L. Manakov, S. I. Marmo, Laser Phys., **7**, 781 (1997).
[36] A. M. Popov, O. V. Tikhonova, and E. A. Volkova, Laser Phys. **10**, 188 (2000).
[37] M.Richter, S.Patchkovskii, F.Morales, O.Smirnova, and M.Ivanov, New J. Phys., **15**, 083012 (2013).
[38] The probability of excitation is the total probability of the population of all the bound states except of the initial (ground) one.
[39] In our case the number of photons coupling the initial ground state and high-level Rydberg states is about 20 and even more.